Nuclear quadrupole relaxation of ^{140}Ce implanted in highly oriented pyrolytic graphite

W. Sato,[1] H. Ueno,[2] A. Taniguchi,[3] Y. Itsuki,[1] Y. Kasamatsu,[4] A. Shinohara,[1] K. Asahi,[2,5] K. Asai,[6] and Y. Ohkubo[3]
[1]*Graduate School of Science, Osaka University, Toyonaka, Osaka 560-0043, Japan*
[2]*Applied Nuclear Physics Laboratory, RIKEN, Wako, Saitama 351-0198, Japan*
[3]*Research Reactor Institute, Kyoto University, Kumatori, Osaka 590-0494, Japan*
[4]*Japan Atomic Energy Agency, Tokai, Ibaraki 319-1195, Japan*
[5]*Department of Physics, Tokyo Institute of Technology, Meguro, Tokyo 152-8551, Japan*
[6]*Department of Applied Physics and Chemistry, The University of Electro-Communications, Chofu, Tokyo 182-8585, Japan*
(Received 11 July 2006; revised manuscript received 22 September 2006; published 13 December 2006)

Nuclear quadrupole relaxation was observed for extremely dilute ^{140}Ce ions implanted in highly oriented pyrolytic graphite by means of the time-differential perturbed angular correlation technique. The temperature-dependent relaxation of the directional anisotropy implies a thermally activated motion of the probe nuclei relative to the extranuclear field with the activation energy of 0.029(3) eV. As regards the electronic property, it is strongly suggested from a measurement under an external magnetic field that the ^{140}Ce ions in motion are in the state of Ce^{3+}.

DOI: 10.1103/PhysRevB.74.214302 PACS number(s): 85.40.Ry, 81.05.Uw, 76.80.+y

I. INTRODUCTION

Interaction between metal and carbon atoms in matter is one of the most important and intriguing subjects in current condensed matter physics and chemistry. Because compounds of such systems, represented by organometallic compounds and graphite intercalation compounds, have great potential for a wide variety of technological applications, their structural and electronic properties have been extensively studied with various spectroscopic techniques.[1] In addition to those static properties, information on the dynamic aspects of their interactions can also be a great help to provide insight into the interacting nature between metal and carbon atoms. In recent years, we have worked on physical properties of endohedral cerium fullerenes, successfully observing intramolecular dynamic motion of the encapsulated Ce atoms relative to the ambient carbons forming a spherical cage structure.[2,3] In a subsequent work for Ce-implanted granular diamond, however, a static Ce-carbon interaction was observed to the contrary.[4] It is obvious from these experimental results that the behavior of Ce ions differs appreciably depending on the structure of the host material.

Relative to these contrasting observations, it is interesting to see what happens if Ce atoms are introduced in graphite, another form of carbon allotropes. As regards dynamics of intercalants, for instance, Zabel *et al.* succeeded in observing diffusion of intercalant alkali-metal atoms (Li, K, Rb, and Cs) in graphite by the quasielastic neutron scattering technique, estimating the diffusion constants and activation energies for each of the atoms.[5] They reported the dependence of those values on the metal atom concentration, which is characterized by their stage index n ($n \geq 1$). Considering the concentration dependence of the mobility of intercalant metal atoms, it is also interesting to examine the case for the extremely dilute limit, which may lead to understanding part of the intrinsic nature of graphite intercalation compounds.

From this point of view, in the present work, we have studied the behavior of isolated Ce isotopes, ^{140}Ce, as impurities implanted in a sheet of highly oriented pyrolytic graphite (HOPG) by means of the time-differential perturbed angular correlation (TDPAC) method. This technique is a powerful spectroscopy for investigation of condensed matter physics as well as nuclear physics.[6,7] It provides invaluable microscopic information on local fields in matter through hyperfine interactions between probe nuclei and the surrounding spins and charge distribution. By observing the time-variant directional anisotropy of γ rays emitted by the disintegration of the excited nuclei of the probes, we can obtain direct information concerning the extranuclear field; that is, this method allows evaluating the magnitude of the hyperfine magnetic field and electric field gradient (EFG) at the site of the probe nucleus, and/or even the nuclear relaxation time, which reflect the local magnetism, structure, and dynamics of the host material.[8] Another notable advantage is that the TDPAC method can provide onsite information about certain isotopes which are difficult or even impossible to be investigated by other spectroscopies, because of the feasibility of selecting suitable nuclear states having inherent electromagnetic moments. Cerium-140 is typical of those isotopes. Because the nuclear spins at the ground states of the stable Ce isotopes are zero, nuclear magnetic resonance and nuclear quadrupole resonance methods, for instance, cannot be applied with the element.

Taking these advantages of this spectroscopy, the dynamic nature and electronic property of the implanted Ce ions are discussed based on the attenuating trend of the directional anisotropy of observed perturbation functions. In the present paper, we propose that the observed nuclear quadrupole relaxation be caused by a thermally activated dynamic motion of the probe Ce ions.

II. EXPERIMENT

A sheet of HOPG with a size of approximately 6 mm $\phi \times 1$ mm was stuck on a Teflon-sheet backing of $10 \times 10 \times 1$ mm^3, and then attached to the ion beam collector equipped at the isotope separator on-line installed at Kyoto University Reactor (KUR-ISOL). Fission products derived

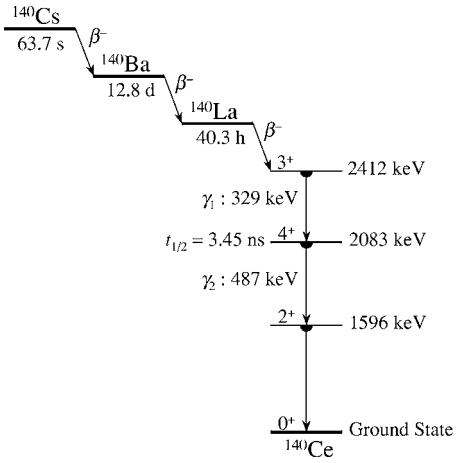

FIG. 1. Simplified decay scheme of ^{140}Ce formed in the disintegration of ^{140}Cs.

from an enriched ^{235}U target in the chamber were rapidly transported into the ion source equipped outside the reactor. After surface ionization, they were accelerated by the acceleration voltage up to 30 kV and were mass separated by the analyzer magnet. The ion beam of interest, ^{140}Cs, was reaccelerated by the acceleration voltage of 70 kV and was kept implanted in the HOPG sample for approximately 30 h. The number of the implanted ^{140}Cs atoms was estimated to be approximately 1.6×10^{11} in total. Detailed description and schematic diagrams of the system of KUR-ISOL appear elsewhere.[9,10] The probe nucleus ^{140}Ce is generated through the disintegration process shown in Fig. 1.[11] It was confirmed by a γ-ray spectrum of the implanted sample that the projectile was well isolated in the mass-separation process.

The irradiated sample underwent a heat treatment at 873 K for 2 h in an atmosphere of argon gas flow at a rate of 1.5 L min^{-1}. After radioactive equilibrium between ^{140}Ba and ^{140}La was achieved, TDPAC measurements were performed at various temperatures from 10 K up to 773 K for the probe ^{140}Ce on the 329–487 keV cascade γ rays with the intermediate state of $I^{\pi}=4^{+}$ having a half-life of 3.5 ns. In the present work, the directional anisotropy of the angular correlations of the cascade γ rays was observed at $\pi/2$- and π-radian directions with a conventional four-detector system. Apart from the measurements above, we carried out TDPAC measurements at 298 K under an external magnetic field of $B_{\mathrm{ext}}=0.84$ T applied perpendicular to the detector plane. Since HOPG is a pseudosingle crystal with the c axis normal to the graphite layers, it was expected that a sample-to-detector configuration dependence might appear in TDPAC spectra, as observed for another experiment performed with a different probe.[12] The sample was therefore placed in two different directions toward the detector plane so that the two-dimensional layers would be parallel to the detector plane (configuration I), and that the layers would be perpendicular to the detector plane, in which each detector is directed so as to face the HOPG layer at $\pi/4$ radians (configuration II), as depicted in Figs. 2(a) and 2(b), respectively. For the coincidence detection, BaF_2 scintillation detectors with 1.5 in. $\phi\times1$ in. pure crystal were adopted; the time resolution of the present system was estimated to be 500 to 600 ps based on the full width at half maximum of the peaks for prompt coincidence. As regards solid angle correction for the γ-ray detection, this work followed a method developed by Lawson and Frauenfelder.[13]

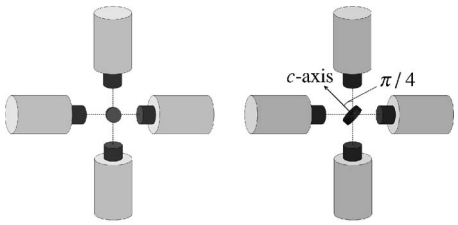

(a) Configuration I (b) Configuration II

FIG. 2. Schematic configurations of the HOPG sample and BaF_2 scintillation detectors.

III. RESULTS AND DATA ANALYSIS

If the principal axis of the EFG at the probe nucleus site is oriented to a certain fixed direction in the laboratory system, there should be a sample-to-detector dependence in the time evolution of the directional anisotropy in the case of static electric quadrupole interaction, as has been observed in the TDPAC measurements with another probe implanted in HOPG.[12] In the present case of $I=4$, the perturbation factors for a single crystalline sample are then theoretically deduced for different orientations of the principal axis of axially symmetric EFGs around the c axis of HOPG as

$$G_{22}^{11}(t)=\frac{1}{462}[10\cos(3\omega_Q t)+81\cos(9\omega_Q t)+175\cos(15\omega_Q t)+196\cos(21\omega_Q t)] \quad (1)$$

and

$$G_{22}^{22}(t)=\frac{1}{231}[50+90\cos(12\omega_Q t)+63\cos(24\omega_Q t)+28\cos(36\omega_Q t)], \quad (2)$$

where $G_{22}^{NN}(t)$ represents the time-differential perturbation factor, t the time interval between the emissions of the cascade γ rays, and ω_Q the nuclear quadrupole frequency related to the principal axis of the EFG, V_{zz}, by

$$\omega_Q=\frac{eQ|V_{zz}|}{4I(2I-1)\hbar}. \quad (3)$$

Here, Q [=0.35 (7) b for the relevant case[11]] is the nuclear quadrupole moment of the intermediate state. Because of the angular dependence of the spherical harmonics, $N=1$ for the case that the principal axis of the EFG is parallel to the detector plane, directing at an angle of $\pi/4$ radians with respect to each detector, and $N=2$ for the EFG axis being perpendicular to the detector plane. Data processing to deduce the time-variant directional anisotropy with the following simple arithmetic operation,

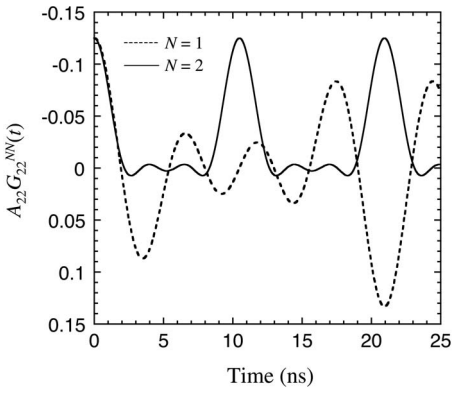

FIG. 3. Simulated time-differential perturbation patterns on the assumption that the probe is in a single crystal. The nuclear quadrupole frequency is assumed to be $\omega_Q = 5 \times 10^7$ rad s^{-1}. The angular correlation coefficient is fixed to the value of $A_{22} = -0.125$. For the explanation of the two lines, see the text.

$$R(t) = \frac{2[N(\pi,t) - N(\pi/2,t)]}{N(\pi,t) + 2N(\pi/2,t)}, \tag{4}$$

gives $R(t) \approx A_{22}G_{22}^{11}(t)$ and $R(t) \approx A_{22}G_{22}^{22}(t)$ for the above cases of $N=1$ and $N=2$, respectively. Here, A_{22} denotes the angular correlation coefficient and $N(\theta, t)$ is the number of the coincident events observed at an angle, θ. Figure 3 shows simulated perturbation patterns for the fixed values, $A_{22} = -0.125$ and $\omega_Q = 5 \times 10^7$ rad s^{-1}, as functions of the time interval between the cascade γ-ray emissions. An apparent configuration dependence can be seen in the way of time evolutions. Observed TDPAC spectra of ^{140}Ce for the measurements at 10 and 298 K are, however, completely different from the above expectation, as shown in Fig. 4. One can see little configuration dependence in the spectra at both temperatures in spite of the different c-axis orientations against

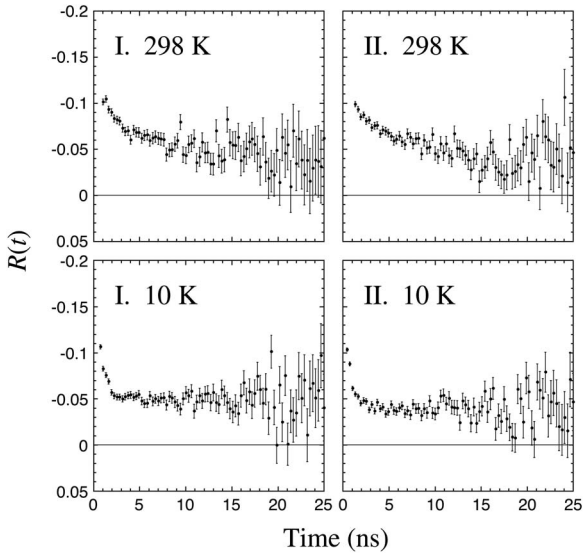

FIG. 4. TDPAC spectra of ^{140}Ce in HOPG at 10 and 298 K. The roman numerals in the figures correspond to the sample-to-detector configurations in Fig. 2.

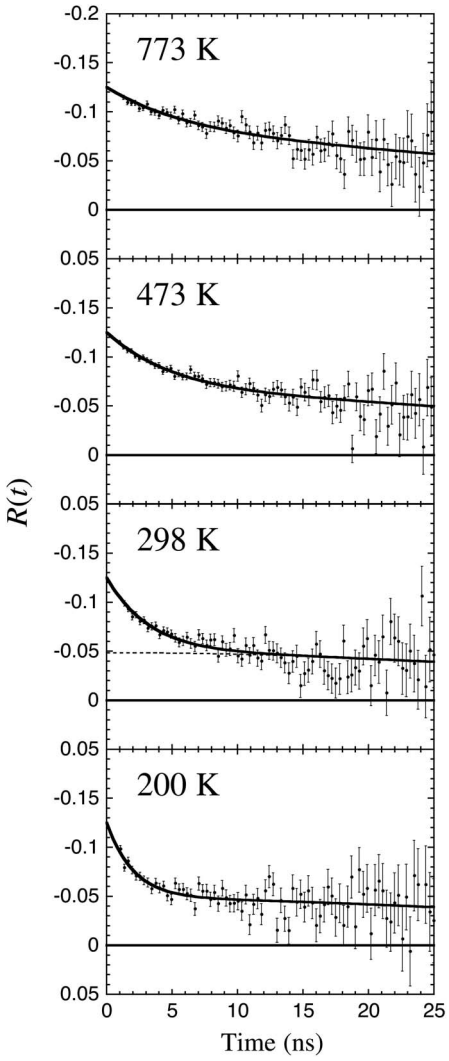

FIG. 5. TDPAC spectra of ^{140}Ce in HOPG at various temperatures. All the spectra are fitted with Eq. (6). As an example, the contribution from the second component is shown by a dotted line in the 298 K spectrum.

the detector plane. It is also obvious in Fig. 4 that the perturbation functions show a gradual relaxation having little oscillating structure. In the present work, therefore, we treat all the data as those for a polycrystalline sample hereafter. (As a cause of the little configuration dependence, it is conceivable that the probe ions reside in defects presumably produced by annealing. However, we actually carried out TDPAC measurements at various temperatures for the same HOPG sample before annealing as well, and have found that the TDPAC spectra show no discernable distinction from the ones obtained after the thermal treatment. It is considered therefore that the production of defects by the annealing, if any, does not affect the experimental results.)

In Fig. 5 are shown TDPAC spectra obtained at a temperature range of 200–773 K for configuration II, which was selected for analysis and discussion because of better counting statistics than those of configuration I. For each spectrum, an exponential-type attenuation in the directional anisotropy can be observed. In spite of relatively fast

attenuation especially at low temperature, however, the angular correlation does not become isotropic completely even after considerably long elapsing time at the intermediate state of the cascade γ-ray emissions. Because it is impossible to fit each spectrum with a single decaying component, we thus regard all the spectra as consisting of two different components: The first one decays exponentially and the second makes a backgroundlike plateau. Since the second component shows a slight attenuation of the anisotropy having little temperature dependence in the present temperature range, we assume a very weak static electric quadrupole interaction for this component[14] as those experimentally observed for some inorganic compounds.[15–20] For a polycrystalline sample, the static time-differential perturbation factor, $G_{22}^{\text{static}}(t)$, for the present case of $I=4$ is explicitly expressed as

$$G_{22}^{\text{static}}(t) = \frac{1}{5}[1 + 2G_{22}^{11}(t) + 2G_{22}^{22}(t)]$$

$$= \frac{1}{1155}[331 + 10\cos(3\omega_Q t) + 81\cos(9\omega_Q t) + 180\cos(12\omega_Q t) + 175\cos(15\omega_Q t) + 196\cos(21\omega_Q t) + 126\cos(24\omega_Q t) + 56\cos(36\omega_Q t)], \quad (5)$$

in the limited case for an axially symmetric EFG produced at the probe nucleus by the surrounding charge distribution. By fixing the ω_Q for the second component to the optimized average value, 1.5×10^6 rad s^{-1},[21] least-squares fits were performed by

$$R(t) = A_{22}[f\exp(-\lambda t) + (1-f)G_{22}^{\text{static2}}(t)]. \quad (6)$$

Here, f is the fraction of the first component and λ is the relaxation constant. The superior numeric 2 in the perturbation factor, $G_{22}^{\text{static2}}(t)$, denotes the second component. We employed a fixed value for the angular correlation coefficient, $A_{22}=-0.125$, for the fits of all the spectra, which was experimentally determined in our previous work[4] for the present detection system in order to quantitatively discuss the relaxation rate of the directional anisotropy. The fraction of the first component was around 60% for all the spectra.

IV. DISCUSSION

A. Origin of the nuclear relaxation

As shown in Fig. 5, gradual attenuation of the directional anisotropy is manifest for this temperature range. Two different mechanisms are conceivable for the interpretation of the relaxation phenomenon: (a) An ensemble of multiple components of different static EFGs and (b) a dynamic perturbation acting on the probe nucleus through the fluctuation of the extranuclear field. As to the first candidate for the relaxation mechanism, simulated perturbation functions of widely distributed nuclear quadrupole frequencies were tentatively drawn for wide ranged centroid values. None of them reproduce the data, however, except for the case that unusual field broadening is assumed. Even if we accept the fit with a huge distribution, it is still difficult to rationalize the temperature dependence of the relaxation rate because the observations are opposite to an intuitive understanding that the field averaging should be attained as temperature becomes higher.

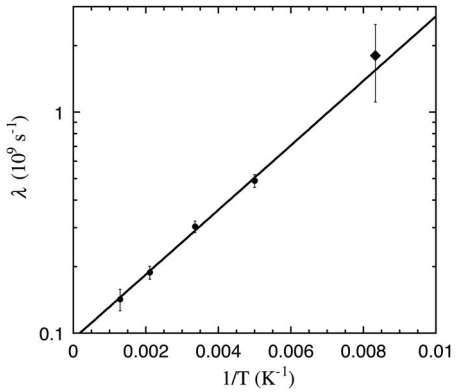

FIG. 6. Temperature dependence of the relaxation constant, λ, for the spectra at high temperatures (solid circles) and at 120 K (a solid diamond). An Arrhenius-type equation, Eq. (8), is used for the fit.

We accordingly assign the origin of the nuclear relaxation phenomenon to the dynamic perturbation from the extranuclear field. This interpretation is based on the diffusion approximation theoretically formulated by Abragam and Pound:[22] The directional anisotropy shows exponential relaxation, as expressed for the first component in Eq. (6), with a time-differential perturbation factor,

$$G_{22}^{\text{dynamic}}(t) = \exp(-\lambda t), \quad (7)$$

when the correlation time of the extranuclear field is sufficiently shorter than $1/\omega_Q$. It is evident from this point of view that the temperature dependence of the relaxation rate suggests a thermally activated motion of the probe nucleus relative to the extranuclear charge distribution. From the following circumstantial evidences, (i) incident Cs^+ ions implanted in HOPG are reported to be intercalated between the graphite basal planes[23] and (ii) jumping diffusion of alkali-metal atoms has been observed for graphite intercalation compounds,[5] we can infer that the present observation also suggests a thermal motion of the implanted impurities among potential wells of the graphite substrate. The relaxation rate rises as temperature falls down, which signifies that the reorientational motion of the EFG at the probe becomes slow.

For detailed investigation of the temperature dependence of the relaxation rate, the relaxation constant, λ, of the first component was plotted as a function of a reciprocal temperature in Fig. 6. A least-squares fitting was carried out for the plotted points assuming an Arrhenius-type equation

$$\lambda = A\exp\left(\frac{E_a}{k_B T}\right), \quad (8)$$

where E_a denotes the activation energy, which was optimized to be 0.029(3) eV. The E_a value [0.029(3) eV] of the relaxation constant hence corresponds to the activation energy for the dynamic motion of the probe nuclei, because the λ is regarded to be proportional to the correlation time, τ_c, for the reorientation of the principal axis of the EFG at the probe

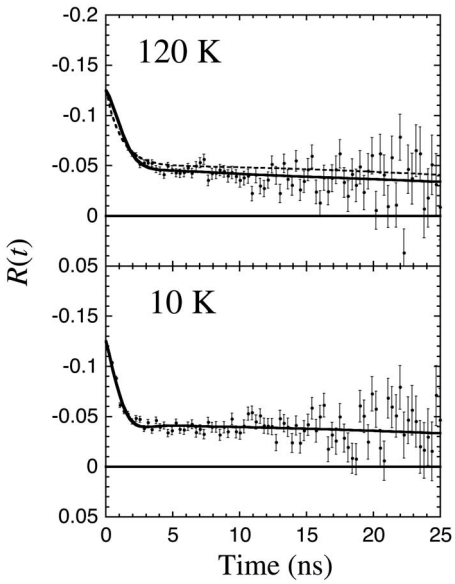

FIG. 7. TDPAC spectra of ^{140}Ce in HOPG at 10 and 120 K. Both spectra are fitted with Eq. (9) (solid lines). The dotted line in the 120 K spectrum is the result of a fit with Eq. (6), which does not reproduce well the time evolution.

nucleus. This value is a little small but comparable with those for the alkali metals in graphite:[5] 0.126, 0.063, and 0.077 eV for KC_{24}, RbC_{24}, and CsC_{24}, respectively. The small value might imply a higher mobility of the dilute impurities free from mutual interference, although the elemental difference cannot be excluded as the reason.

Further investigation of the attenuating trend of the directional anisotropy at lower temperature was performed in order to examine the validity of the above interpretation on the nuclear relaxation. Figure 7 shows TDPAC spectra at 10 and 120 K. As indicated by the dotted line in 120 K spectrum, it is difficult to reproduce with Eq. (6) the data showing this prompt damping. The directional anisotropies in this slow fluctuation regime were, therefore, fitted by employing an adiabatic approximation[24] of a quasistatic perturbation for the first component with

$$R(t) = A_{22}[f \exp(-t/\tau_c) G_{22}^{\text{static1}}(t) + (1-f) G_{22}^{\text{static2}}(t)]. \quad (9)$$

It is to be noted that a fit without the damping exponential prefactor for the first component does not reproduce the data unless an unusually broad distribution is assumed for the nuclear quadrupole frequency. The ω_Q and τ_c values for the first component were estimated to be $4.2(5) \times 10^7$ rad s^{-1} and 3.9(15) ns for 120 K spectrum and $6.2(6) \times 10^7$ rad s^{-1} and 2.3(5) ns for 10 K spectrum, respectively. The fraction of the first component was around 65% for both of the spectra. In order to corroborate the above analytical method, the λ value for the 120 K spectrum is indicated as well by a different symbol (solid diamond) in Fig. 6, which was deduced with[22]

$$\lambda = \frac{3}{5} \tau_c \omega_Q^2 k(k+1)[4I(I+1) - k(k+1) - 1], \quad (10)$$

where ω_Q is the nuclear quadrupole frequency at the relevant temperature for the first component obtained by the fit with Eq. (9). For the present study, $k=2$. The interpretation of the first component by the fits with Eqs. (6) and (9) is supported by a smooth continuity of the λ values. Considering the trend of the temperature dependence, we reasonably expect a completely static perturbation for the first component because of freezing of the thermal motion at temperature as low as 10 K. As is evident from the τ_c value optimized by the least-squares fit, however, the probe nucleus still experiences a slow dynamic perturbation as expressed by the damping exponential prefactor of Eq. (9). (It should be noted here again that an unusually broad distribution has to be assumed for the quadrupole frequency to fit the data without the damping prefactor.) This fast damping may imply some different mechanism(s) functioning at this temperature other than the thermal motion: One of the candidates is, for example, a temperature-independent motion of the probe atoms triggered by the recoil effect of the β particle emission from the parent ^{140}La nuclei, as concluded in our previous work for endohedral Ce atoms in fullerene cages.[2–4]

As another origin of the nuclear relaxation of ^{140}Ce, we should take into consideration the effect of hyperfine magnetic interaction with a localized $4f$ spin in a paramagnetic Ce^{3+}, as has been observed in metal hosts.[25–27] Without an external magnetic field ($B_{\text{ext}}=0$) just as the case for the present measurements, the effective magnetic field averaged over nuclei in paramagnetic atoms is considered to be zero ($B_{\text{eff}}=0$) in general. However, the instantaneous hyperfine field at a Ce nucleus in the presence of a $4f$ electron is so large [$B(0) \sim 180$ T (Refs. 25, 28, and 29)] that the finite fast fluctuation of the paramagnetic $4f$ spin might make a contribution to the observed nuclear relaxation. In order to examine this possibility, we have thus attempted to fit the 10 and 120 K spectra applying the same analytical method with the adiabatic approximation as employed for the quadrupole interaction using a fixed Larmor frequency of $\omega_L = 9.4 \times 10^9$ rad s^{-1}, which is estimated from the $B(0)$. Because the instantaneous magnetic field is enormous and independent of temperature,[6,22] however, the data could not be reproduced by any means. For the present observations, therefore, the nuclear relaxation is not ascribable to the $4f$ spin fluctuation.

B. Electronic states of ^{140}Ce

Referring to several experimental observations reported for ^{140}Ce, we give here an interpretation to the oxidation state of the dilute Ce ions. After β^- disintegration of a trivalent La^{3+}, the daughter nuclide is reported to take the tetravalent state, Ce^{4+}, in some inorganic compounds,[15–20] and the estimated EFG values for $^{140}Ce^{4+}$ are in the order of 10^{17} V cm^{-2}; in such cases, as is evident from the second component of the present data, the directional anisotropy hardly show a drastic change by this small field during the present time window of ~20 ns. We accordingly propose that the present fast nuclear relaxation be due to a large electromagnetic field produced by a $4f$ electron in the state of Ce^{3+}. There should be a large contribution to the quadrupole interaction from a $4f$ electron itself and the distortion of the charge distribution of the inner closed shell caused by the $4f$ electron. In the same way as the case for the electron rear-

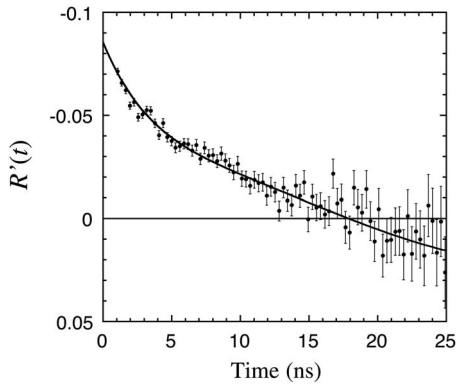

FIG. 8. TDPAC spectrum of ^{140}Ce in HOPG at 298 K. An external magnetic field of B_{ext}=0.84 T perpendicular to the detector plane is applied. The spectrum is fitted with Eq. (12).

rangement in metal, which is known to be completed within a time shorter than 10^{-12} s, the valence state of the probe is considered to have become trivalent through a prompt reductive contribution from π electrons delocalizing in the sp^2 hybridized orbital.

For the second component, the optimized EFG value, 3.2×10^{17} V cm^{-2}, is as small as those for the above cited inorganic compounds. It seems reasonable to infer by analogy with the cases for the inorganic compounds that the Ce ions for the second component take the state of Ce^{4+}. Because the probe ions were kinetically introduced into the host HOPG, there is a strong possibility that the implantation process causes damages in the lattice; the structure with a conjugated network of π orbital might have been destroyed by the formation of dangling bonds at the sites where the projectiles stopped. As a result, the reducing atmosphere of the π orbital is reduced, and the Ce ions would remain tetravalent after the β^- decay.

In order to corroborate this interpretation, we performed a TDPAC measurement at room temperature for the same sample applying an external magnetic field of 0.84 T. The time-dependent perturbation function, $R'(t)$, was obtained by the following operation for the coincident events:

$$R'(t) = \frac{N(\pi,t) - N(\pi/2,t)}{N(\pi,t) + N(\pi/2,t)}. \tag{11}$$

As shown in Fig. 8, the effect of the magnetic field can be seen in the rotational nature of the directional anisotropy. Following our inference on the respective charge states as Ce^{3+} and Ce^{4+} for the first and second components, the TDPAC function was fitted by least squares with

$$R'(t) = \frac{3}{4}A_{22}[f\cos(2\beta\omega_L t)\exp(-\lambda t) + (1-f)\cos(2\omega_L t)G_{22}^{\text{static2}}(t)], \tag{12}$$

where ω_L is the Larmor frequency with the externally applied magnetic field and β denotes the paramagnetic correction factor,[30,31] which is introduced for the correction of enhancement of magnetic induction arising from a small polarization when an external magnetic field is applied to paramagnetic materials. The effective magnetic field is then given as $B_{\text{eff}}=\beta(T)B_{\text{ext}}$. It is to be noted that Eq. (12) holds as an approximation in the present case where $\omega_L \gg \omega_Q$ for the second component. For the present case, ω_L is evaluated from the relation, $\omega_L\hbar = g_N\mu_N B_{\text{ext}}$, as 4.38×10^7 rad s^{-1}, where g_N=1.088.[11] Substituting all the optimized values for the 298 K data in Fig. 5 and this ω_L value for the relevant parameters in Eq. (12), the TDPAC spectrum in Fig. 8 was fitted with Eq. (12). The β value was estimated from the fit to be 1.30(20), which agrees well with those for paramagnetic Ce^{3+} as dilute impurities in metals.[25] This observation strongly supports our proposal on the valence state of the Ce ions for the first component.

V. SUMMARY AND CONCLUSION

The TDPAC technique has been applied to studies of the dynamic and electronic properties of Ce ions as extremely dilute impurities in an HOPG sheet. From the temperature-dependent exponential relaxation of the directional anisotropy of the angular correlations, a thermally activated dynamic motion of the probe nucleus relative to the extranuclear charge distribution was suggested. The activation energy of the dynamic motion, E_a=0.029(3) eV, is comparable with those observed for diffusions of alkali metals in graphite intercalation compounds.[5] As regards the electronic property of the probe, it has been inferred from the large EFG that the first component is in the trivalent state, Ce^{3+}. This inference is evidently supported by the value of the paramagnetic correction factor obtained by a TDPAC measurement under an external magnetic field. The temperature-independent second component possibly corresponds to those occupying sites damaged by the heavy-ion implantation. For more detailed information of this component, another method needs to be developed for soft introduction of an extremely dilute amount of the probe ions so that the sample should be free from lattice defects.

ACKNOWLEDGMENTS

We are grateful to Y. Kawase for his arrangement for the operation of KUR-ISOL. We express our gratitude to T. Saito and Y. Yamaguchi for providing experimental facilities for the TDPAC measurements. We are indebted to Y. Kobayashi and M. K. Kubo for sample preparation. W.S. gratefully acknowledges helpful advice from H. Nakahara, K. Sueki, and H. Ogawa. The present work was accomplished as part of the Visiting Researcher's Program of the Kyoto University Research Reactor Institute (KURRI), and was supported in part by a grant from the Ministry of Education, Culture, Sports, and Science of Japan.

[1] M. S. Dresselhaus and G. Dresselhaus, Adv. Phys. **51**, 1 (2002).
[2] W. Sato, K. Sueki, K. Kikuchi, K. Kobayashi, S. Suzuki, Y. Achiba, H. Nakahara, Y. Ohkubo, F. Ambe, and K. Asai, Phys. Rev. Lett. **80**, 133 (1998).
[3] W. Sato, K. Sueki, K. Kikuchi, S. Suzuki, Y. Achiba, H. Nakahara, Y. Ohkubo, K. Asai, and F. Ambe, Phys. Rev. B **58**, 10850 (1998).
[4] W. Sato, K. Sueki, Y. Achiba, H. Nakahara, Y. Ohkubo, and K. Asai, Phys. Rev. B **63**, 024405 (2001).
[5] H. Zabel, A. Magerl, J. J. Rush, and M. E. Misenheimer, Phys. Rev. B **40**, 7616 (1989).
[6] H. Frauenfelder and R. M. Steffen, in *α-, β-, and γ-Ray Spectroscopy*, edited by K. Siegbahn (North-Holland, Amsterdam, 1965), Vol. 2, p. 997.
[7] G. Schatz and A. Weidinger, *Nuclear Condensed Matter Physics* (John Wiley, New York, 1996).
[8] M. O. Zacate, A. Favrot, and G. S. Collins, Phys. Rev. Lett. **92**, 225901 (2004).
[9] Y. Kawase, K. Okano, and Y. Funakoshi, Nucl. Instrum. Methods Phys. Res. A **241**, 305 (1985).
[10] Y. Kawase, K. Okano, and K. Aoki, Nucl. Instrum. Methods Phys. Res. B **26**, 341 (1987).
[11] *Table of Isotopes*, edited by R. B. Firestone and V. S. Shirley (Wiley, New York, 1996), Vol. 1, 8th ed.
[12] W. Sato *et al.* (unpublished).
[13] J. S. Lawson, Jr. and H. Frauenfelder, Phys. Rev. **91**, 649 (1953).
[14] The interpretation of this component is somewhat different from that given in our previous work (Ref. 4). By detailed examination in the present wide temperature range with better counting statistics, it has been found that there is no systematic temperature dependence for the relevant component. We thus assume here an electrostatic perturbation rather than an exponential decay for this component.
[15] R. M. Levy and D. A. Shirley, Phys. Lett. **3**, 46 (1962).
[16] N. Kaplan, S. Ofer, and B. Rosner, Phys. Lett. **3**, 291 (1963).
[17] H. J. Körner, E. Gerdau, C. Günther, K. Auerbach, G. Mielken, G. Strube, and E. Bodenstedt, Z. Phys. **173**, 203 (1963).
[18] M. Schmorak, H. Wilson, P. Gatti, and L. Grodzins, Phys. Rev. **134**, B718 (1964).
[19] B. Klemme and H. Miemczyk, J. Phys. Soc. Jpn. **34**, 265 (1973).
[20] P. Herzog, B. Klemme, and G. Schäfer, Z. Phys. **269**, 265 (1974).
[21] We first fit Eq. (6) to each data without fixing the ω_Q of the second component treating as a free parameter. The optimization was then performed by averaging each of the obtained values with a small statistic variation.
[22] A. Abragam and R. V. Pound, Phys. Rev. **92**, 943 (1953).
[23] Y. Zhu, J. D. McBride, T. A. Hansen, and T. P. Beede, Jr., J. Phys. Chem. B **105**, 2010 (2001).
[24] A. G. Marshall and C. F. Meares, J. Chem. Phys. **56**, 1226 (1972).
[25] V. V. Krishnamurthy, S. N. Mishra, M. R. Press, and S. H. Devare, Phys. Rev. Lett. **74**, 1661 (1995).
[26] M. Luszik-Bhadra, H. J. Barth, H. J. Brocksch, G. Netz, D. Riegel, and H. H. Bertschat, Phys. Rev. Lett. **47**, 871 (1981).
[27] D. Riegel, Phys. Rev. Lett. **48**, 516 (1982).
[28] H. J. Barth, G. Netz, K. Nishiyama, and D. Riegel, Phys. Rev. Lett. **45**, 1015 (1980).
[29] B. Bleaney, in *Magnetic Properties of Rare Earth Metals*, edited by R. J. Elliott (Plenum, London, 1972), p. 383.
[30] C. Günther and I. Lindgren, in *Perturbed Angular Correlations*, edited by E. Karlsson, E. Matthias, and K. Siegbahn (North-Holland, Amsterdam, 1964), p. 357.
[31] H. J. Barth, M. Luszik-Bhadra, and D. Riegel, Phys. Rev. Lett. **50**, 608 (1983).